

**Electronic Supplementary Information:**

**“Quantum interference in the mechanism of  $H + LiH^+ \rightarrow H_2 + Li^+$  reaction dynamics”**

Jayakrushna Sahoo, Ajay Mohan Singh Rawat and S. Mahapatra<sup>1, a)</sup>

*School of Chemistry, University of Hyderabad, Hyderabad, 500 046,  
India*

---

<sup>a)</sup>Email : susanta.mahapatra@uohyd.ac.in

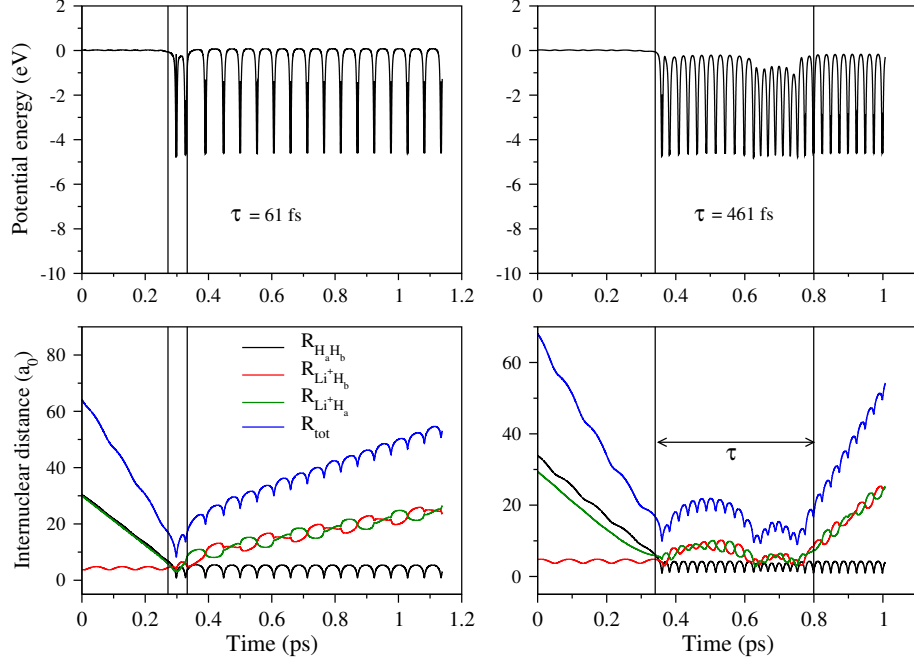


FIG. S1. Typical reactive trajectories of the  $\text{H} + \text{LiH}^+$  ( $v=0, j=0$ )  $\rightarrow \text{H}_2 + \text{Li}^+$  reaction. The solid blue line corresponds to the sum of all three internuclear distances ( $R_{\text{H}_a\text{H}_b} + R_{\text{Li}^+\text{H}_b} + R_{\text{Li}^+\text{H}_a}$ ). The two vertical lines represent the first and last instances of time at which the geometrical criterion, that the sum of all three internuclear distances is  $17 \text{ } a_0$ , is satisfied (see text for details). The total time spent by the trajectory inside these two vertical lines is regarded as the collision time.

TABLE S1. The maximum value of impact parameter ( $b_{\max}$ ) at different collision energies used in the QCT calculation of the  $\text{H} + \text{LiH}^+$  ( $v=0, j=0$ )  $\rightarrow \text{H}_2 + \text{Li}^+$  reaction.

$E_{\text{col}}$ (eV)	$b_{\max}$ ( $a_0$ )
0.005	15.5
0.01	14.0
0.02	12.8
0.03	12.3
0.05	11.7
0.1	11.0
0.2	10.6
0.3	10.3
0.4	10.2
0.5	9.3

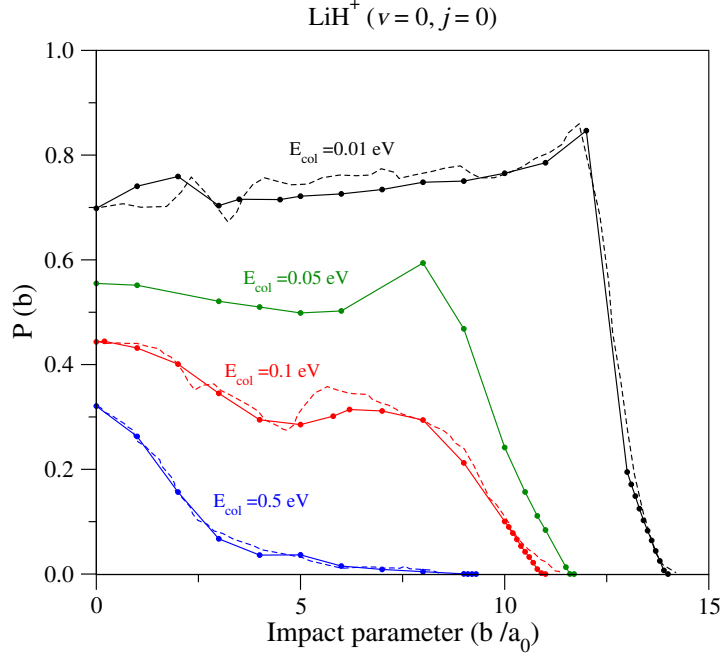


FIG. S2. QCT opacity functions for the  $\text{H} + \text{LiH}^+ (v=0, j=0) \rightarrow \text{H}_2 (v', j') + \text{Li}^+$  reaction at four collision energies. The solid lines with filled circles represent the results of the present QCT calculation and the dashed lines represent the QCT results of Pino *et al.*<sup>1</sup>

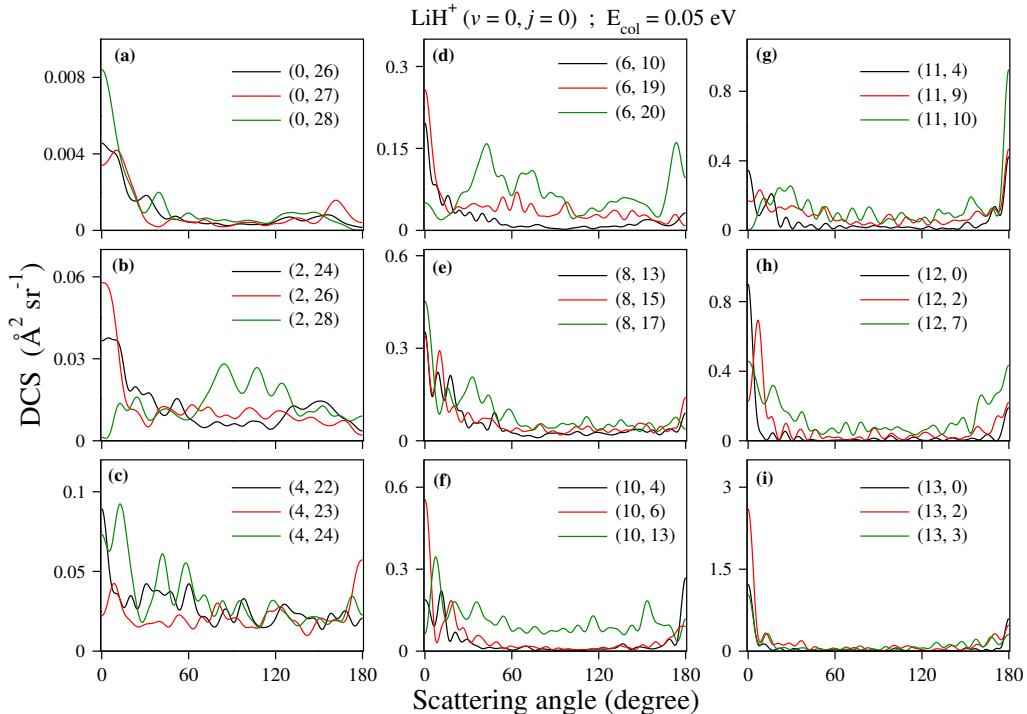


FIG. S3. Product rotational level resolved state-to-state DCS for the  $\text{H} + \text{LiH}^+ (v=0, j=0) \rightarrow \text{H}_2 (v', j') + \text{Li}^+$  reaction as a function of the center-of-mass scattering angle at  $E_{\text{col}} = 0.05$  eV for some selected  $v'$  levels of  $\text{H}_2$ .

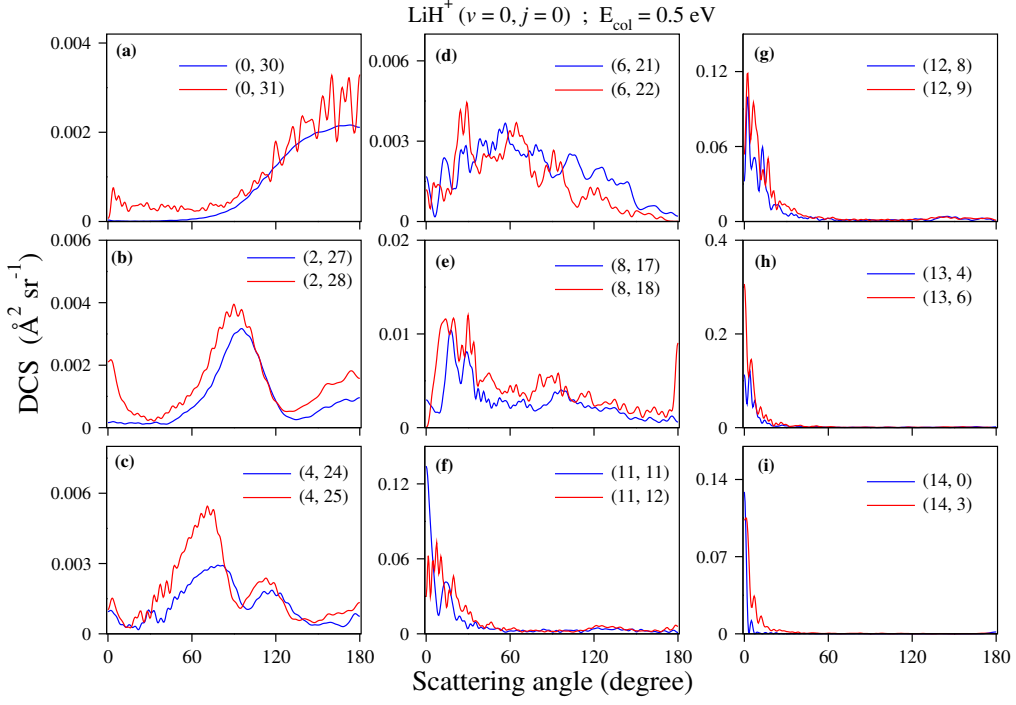


FIG. S4. Same as in Fig. S3, but for  $E_{\text{col}} = 0.5$  eV.

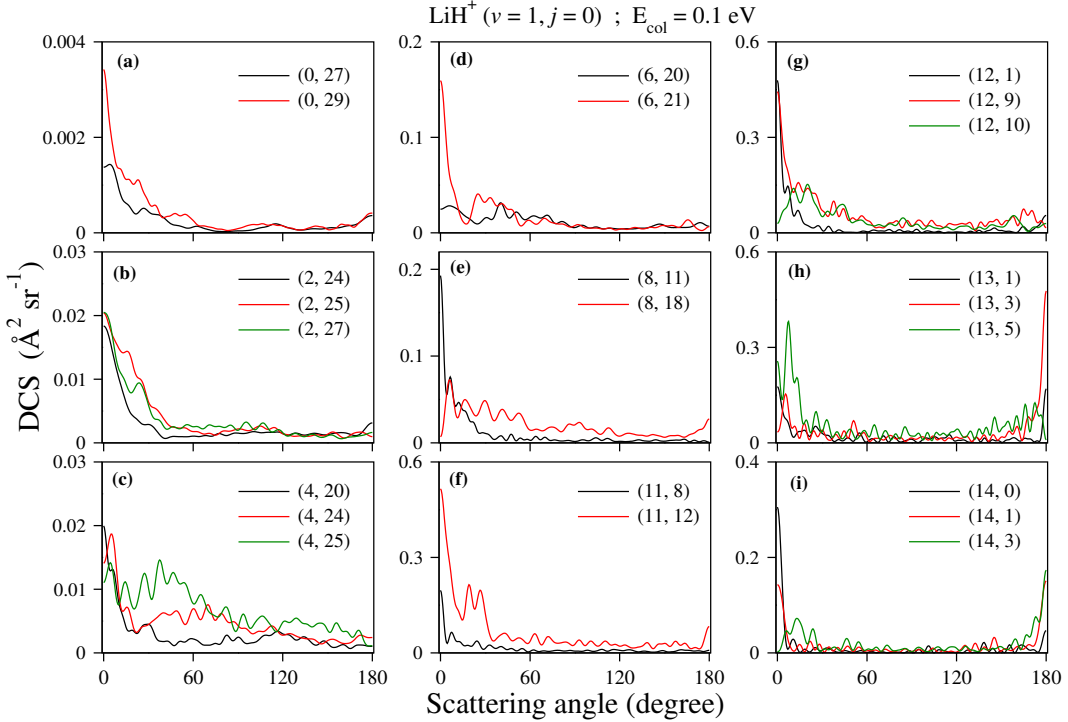


FIG. S5. Product rotational level resolved state-to-state DCS for the  $\text{H} + \text{LiH}^+ (v=1, j=0) \rightarrow \text{H}_2 (v', j') + \text{Li}^+$  reaction as a function of the center-of-mass scattering angle at  $E_{\text{col}} = 0.1$  eV for some selected  $v'$  levels of  $\text{H}_2$ .

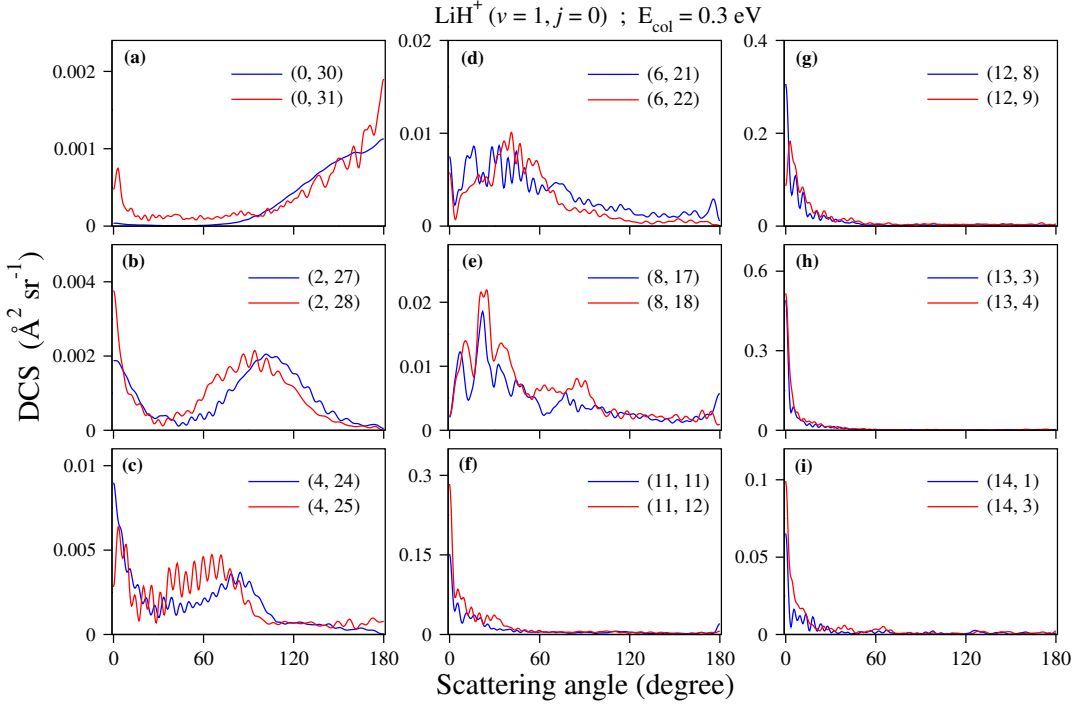


FIG. S6. Same as in Fig. S5, but for  $E_{\text{col}} = 0.3 \text{ eV}$ .

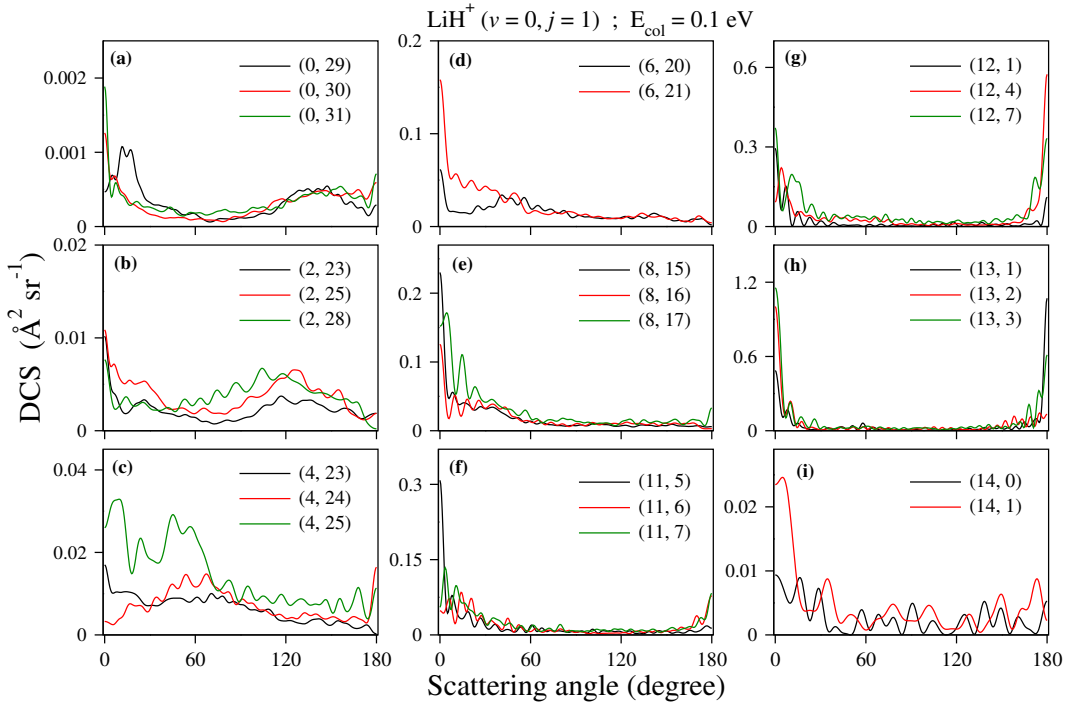


FIG. S7. Product rotational level resolved state-to-state DCS for the  $\text{H} + \text{LiH}^+ (v=0, j=1) \rightarrow \text{H}_2 (v', j') + \text{Li}^+$  reaction as a function of the center-of-mass scattering angle at  $E_{\text{col}} = 0.1 \text{ eV}$  for some selected  $v'$  levels of  $\text{H}_2$ .

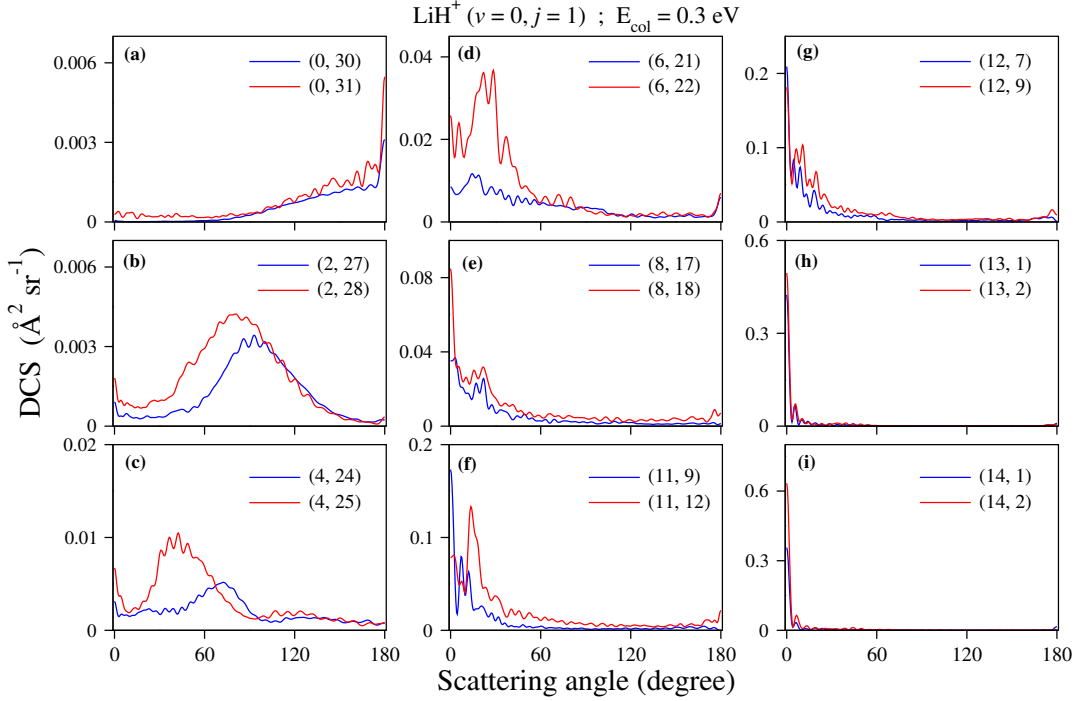


FIG. S8. Same as in Fig. S7, but for  $E_{\text{col}} = 0.3 \text{ eV}$ .

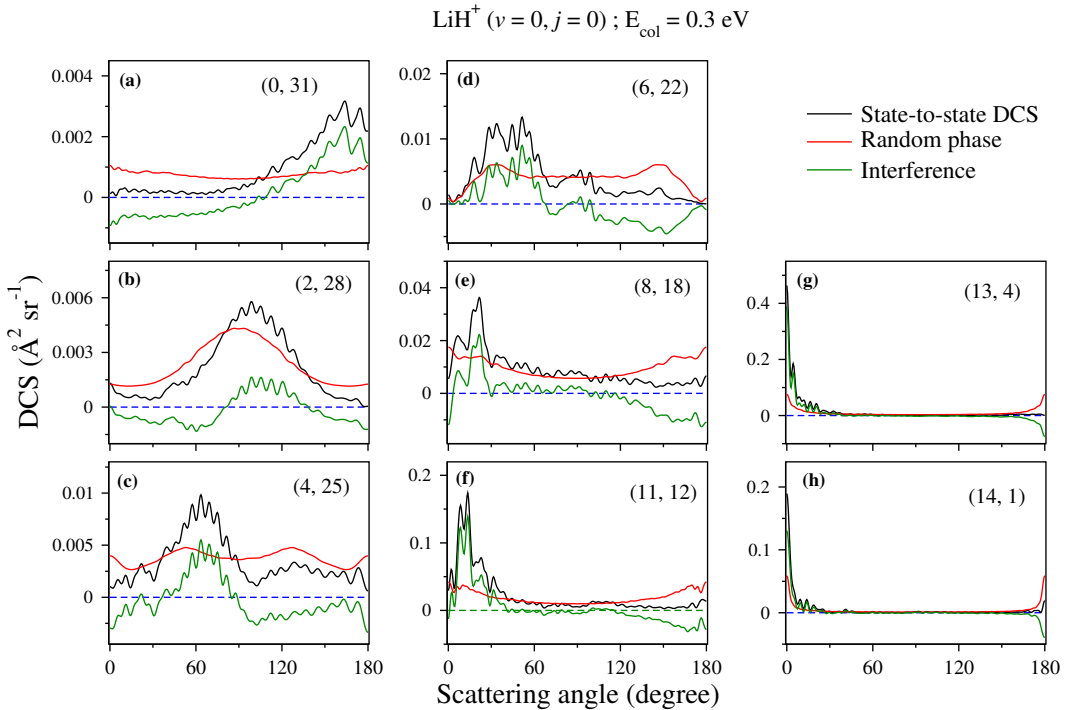


FIG. S9. Product rotational level resolved state-to-state interference terms (green), state-to-state DCSs (black) and DCSs due to RPA (red) for the  $\text{H} + \text{LiH}^+ (v=0, j=0) \rightarrow \text{H}_2 (v', j') + \text{Li}^+$  reaction as a function of scattering angle ( $\theta$ ) at  $E_{\text{col}} = 0.3 \text{ eV}$  for few selected  $(v', j')$  levels of  $\text{H}_2$ . The blue color dashed line along the abscissa represents the zero of the ordinate.

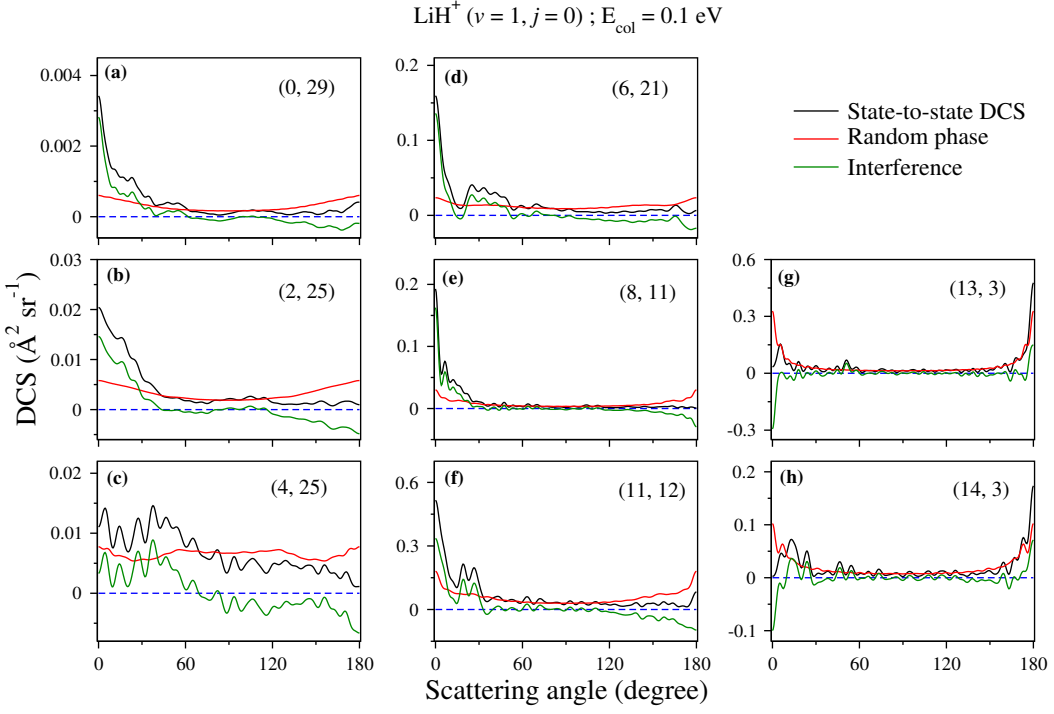


FIG. S10. Same as in Fig. S9, but for the  $\text{H} + \text{LiH}^+ (v=1, j=0) \rightarrow \text{H}_2 (v', j') + \text{Li}^+$  reaction at  $E_{\text{col}} = 0.1 \text{ eV}$ .

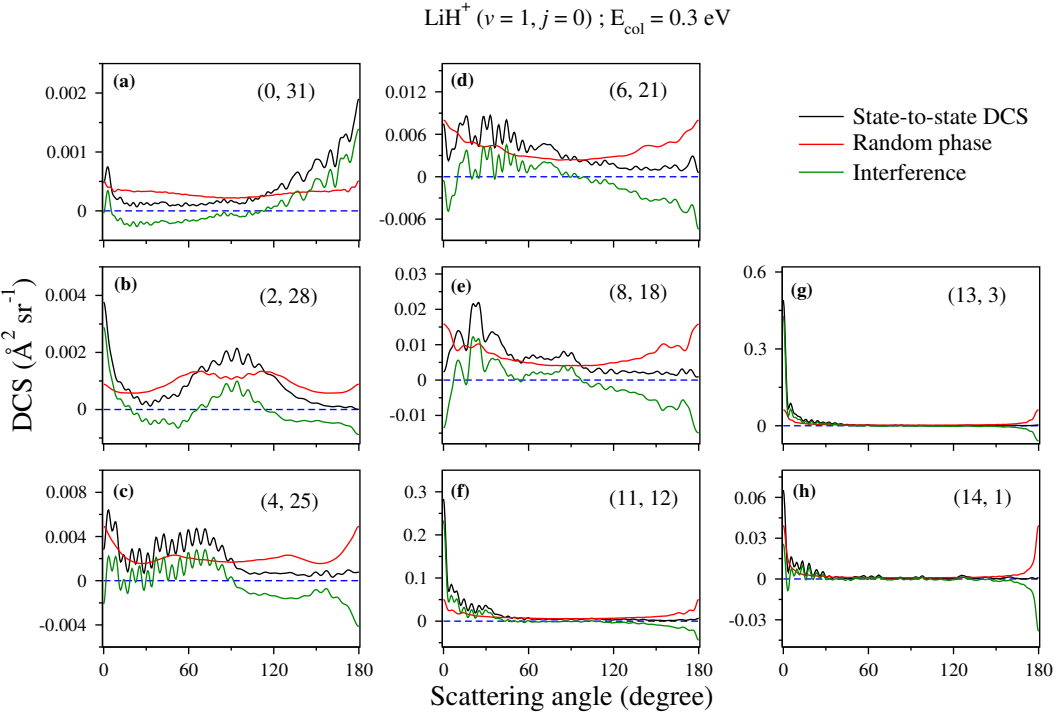


FIG. S11. Same as in Fig. S9, but for the  $\text{H} + \text{LiH}^+ (v=1, j=0) \rightarrow \text{H}_2 (v', j') + \text{Li}^+$  reaction at  $E_{\text{col}} = 0.3 \text{ eV}$ .

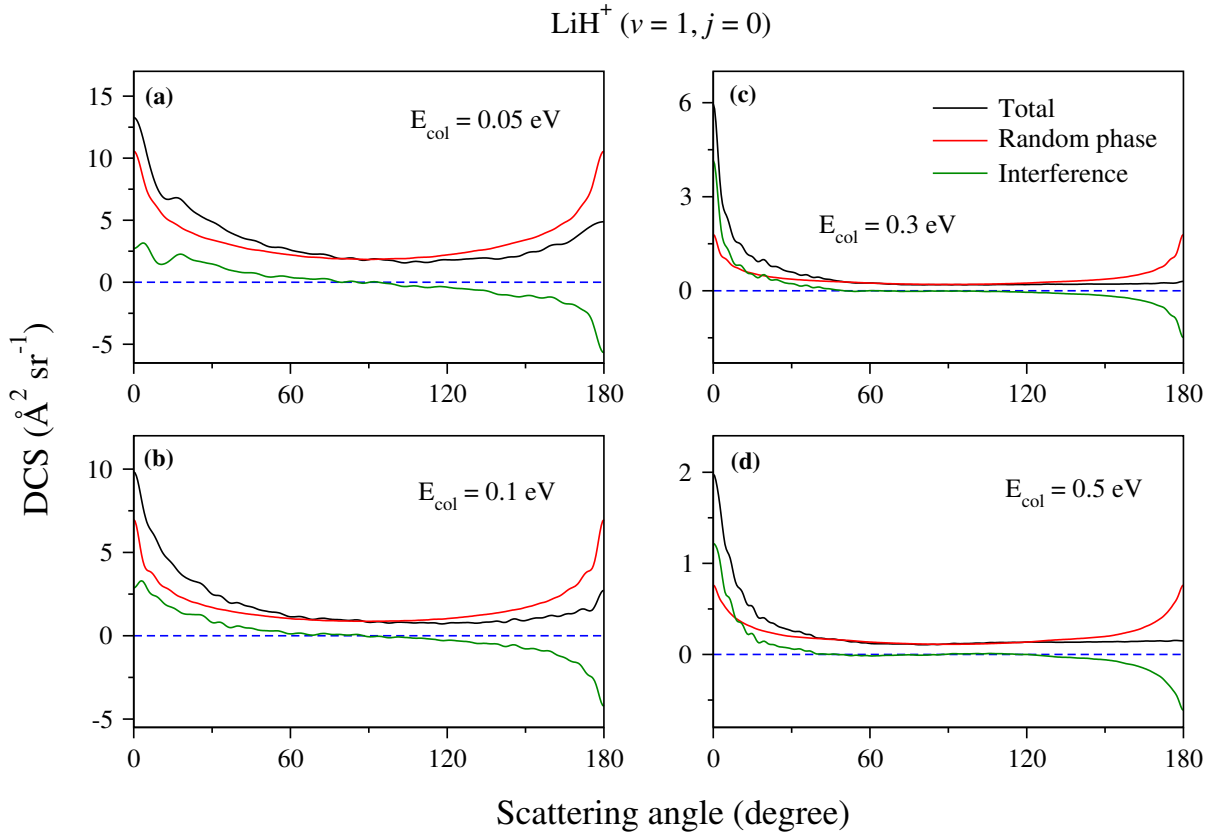


FIG. S12. Total (summed over final states) interference terms (green), total DCSs (black) and DCSs due to RPA (red) for the  $\text{H} + \text{LiH}^+ (\nu=1, j=0) \rightarrow \text{H}_2 (\Sigma\nu', \Sigma j') + \text{Li}^+$  reaction as a function of the scattering angle ( $\theta$ ) at  $E_{\text{col}} = 0.05, 0.1, 0.3$  and  $0.5 \text{ eV}$ . The blue color dashed line along the abscissa represents the zero of the ordinate.

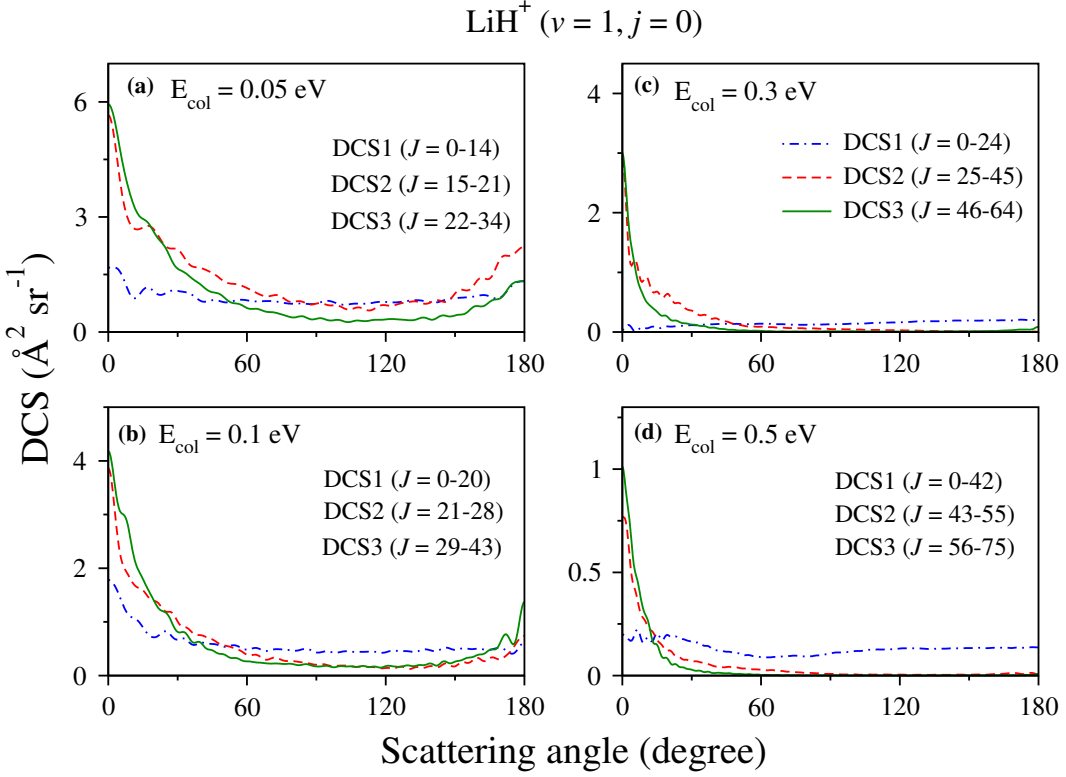


FIG. S13. Initial state-selected partial DCSs (DCS1, DCS2 and DCS3) for the  $\text{H} + \text{LiH}^+ (v=1, j=0) \rightarrow \text{H}_2 (\Sigma v', \Sigma j') + \text{Li}^+$  reaction as a function of scattering angle ( $\theta$ ) at  $E_{\text{col}} = 0.05, 0.1, 0.3$  and  $0.5$  eV. Three different ranges of the chosen partial wave,  $J$ , are mentioned inside each panel. The partial DCSs are shown by different colors and line types.

## **MOVIE 1**

The movie of a representative trajectory for the roaming of the attacking H atom before the formation of product H<sub>2</sub> at E<sub>col</sub> = 0.01 eV. This trajectory corresponds to that shown in Fig. 7(a) of the Main text.

## **MOVIES 2-4**

The movies of three representative trajectories for the roaming of the recoiling Li<sup>+</sup> ion after the formation of product H<sub>2</sub> at E<sub>col</sub> = 0.01 eV. These trajectories, respectively, correspond to those shown in Fig. 7(b)-(d) of the Main text.

## REFERENCES

<sup>1</sup>I. Pino, R. Martinazzo and G. F. Tantardini, *Phys. Chem. Chem. Phys.*, 2008, **10**, 5545–5551.